Experimental and Kinetic Investigations of CO2 Gasification of Fine Chars Separated from a Pilot-Scale Fluidized-Bed Gasifier

ARTICLE *in* ENERGY & FUELS · APRIL 2013

Impact Factor: 2.79 · DOI: 10.1021/ef4002296

6 AUTHORS, INCLUDING:

Zhiqing Wang
Chinese Academy of Sciences
10 PUBLICATIONS **62** CITATIONS

energy&fuels

Article

pubs.acs.org/EF

Experimental and Kinetic Investigations of CO_2 Gasification of Fine Chars Separated from a Pilot-Scale Fluidized-Bed Gasifier

Xuliang Jing,[†,‡] Zhiqing Wang,[†] Zhongliang Yu,[†,‡] Qian Zhang,[†,‡] Chunyu Li,[†] and Yitian Fang*[,†]

[†]State Key Laboratory of Coal Conversion, Institute of Coal Chemistry, Chinese Academy of Sciences, Taiyuan 030001, People's Republic of China

[‡]University of Chinese Academy of Sciences, Beijing 100049, People's Republic of China

ABSTRACT: The CO_2 gasification behaviors of two fine chars separated from a pilot-scale fluidized-bed gasifier were studied in a thermogravimetric analyzer (TGA) within the temperature range of 1000−1300 °C. The physical properties of fine chars were examined by scanning electron microscopy (SEM), N_2 adsorption, and X-ray diffraction (XRD). The differences in gasification reactivity and related properties between the fine chars and the corresponding experimental-produced coal chars were also compared. The results show that the fine chars have higher ash content, larger Brunauer−Emmett−Teller (BET) surface area, and better gasification reactivity than the corresponding coal chars. The gasification reactivity of fine chars was promoted by the catalytic alkali and alkaline earth metals (AAEMs) but inhibited by the enrichment of the ash layer in a higher carbon conversion range or the ash melting at a higher temperature. In addition to the AAEMs, the reactivity of different fine chars is mainly influenced by their pore and carbon crystalline structures. The kinetic investigation reveals that the modified random pore model (MRPM) and shifted-modified random pore model (S-MRPM) perform more reasonably than the random pore model (RPM) in some special conditions. Moreover, the reactivity of fine chars increases, and the reaction shifts from chemical reaction control to gas diffusion control as the gasification temperature increases.

1. INTRODUCTION

Fluidized-bed gasification has been considered as a promising syngas-producing technology because of its wide coal adaptability, effectiveness in the control of pollutant emissions, and lower operational cost.[1,2] However, massive carbon-rich fine chars are entrained out by the syngas, resulting in a lower total carbon conversion (~90%). Thus, the typical fluidized-bed gasifiers, such as the HTW, KRW, U-gas, and transport gasifiers, recirculate the fine chars to the gasifier and reuse them as a feedstock.[3,4] Nevertheless, the fine chars have been partially gasified, and the regasification reactivity is lower. On the other hand, the fine chars have undergone a shorter residence time in the gasifier because of the smaller particle sizes. These factors make the fine chars difficult to be converted in the fluidized-bed gasifier at lower temperatures (900−1000 °C), which has already been verified by the Institute of Coal Chemistry (ICC), Chinese Academy of Sciences (CAS).[5] One solution to this problem is to regasify the fine chars at a higher temperature. The entrained flow gasifier, for example, operates at 1250−1600 °C with a residence time of a few seconds, the carbon conversion of which could be up to 99%.[6] Consequently, a new approach integrating the ash agglomerate fluidized-bed gasifier (AFB) with an entrained flow gasifier was proposed, by which the fine chars from AFB were directly transferred to an entrained flow gasifier and gasified in the temperature range of 1200−1300 °C.[7] Hence, understanding of the gasification behavior of fine chars in this temperature range is essential for actualizing this integration.

However, few attempts have been made to examine the gasification of fine chars derived from a fluidized-bed gasifier at elevated temperatures. It has been investigated that the fly ashes derived from a circulating fluidized-bed combustor have a relatively lower surface area and smooth surface morphology.[8,9] The gasification behaviors of pyrolysis coal chars have also been widely studied.[10−13] These chars are pyrolyzed under an inert atmosphere, while the gasifier fine chars have been partially gasified, oxidized, and activated by steam. These factors make the properties of fine chars markedly different from the fly ashes and coal chars. For example, the anthracite fine char from the fluidized-bed gasifier has a larger surface area and higher carbon crystalline structure,[14] while the entrained flow gasifier fine char exhibits a lower crystalline structure and higher CO_2 gasification reactivity than the rapid pyrolysis coal char.[15] Earlier work by Xu et al.[16] identified the crystalline structure and inherent minerals as the determinants for the gasification reactivity of entrained flow gasifier fine char. The gasification kinetics of fine chars from the AFB has been studied by ICC,[5] but the adopted regasification temperature is lower than 1000 °C, which could not match with the previously mentioned entrained flow gasifier.

The gasification kinetics is essential for the efficient and reliable design of the coal gasification system. Because of the simplicity of design and ease of operation, the thermogravimetric analyzer (TGA) is widely used to obtain the gasification kinetics. In this paper, the CO_2 gasification behaviors of fine chars separated from the pilot-scale AFB were studied by a TGA at temperatures of 1000−1300 °C. The property and reactivity differences between the fine chars and the corresponding coal chars were evaluated. Moreover, the gasification processes were described by the random pore

Received: November 9, 2012
Revised: April 13, 2013
Published: April 15, 2013

   dx.doi.org/10.1021/ef4002296 | *Energy Fuels* 2013, 27, 2422−2430

Table 1. Proximate and Ultimate Analyses of Samples

	proximate analysis (wt %, air-dry basis)				ultimate analysis (wt %, dry and ash-free basis)				
sample	V	M	A	FC	C	H	O[a]	N	S_t
XY coal	8.3	1.6	19.4	70.7	90.2	4.2	3.9	1.2	0.5
YC coal	7.6	1.2	22.2	69.1	89.5	3.0	5.7	1.2	0.5
XYCC	1.1	0.6	19.7	78.6	95.1	1.3	2.2	1.0	0.4
YCCC	2.1	1.1	17.9	78.9	94.7	1.3	2.0	1.1	1.1
XYFC	1.2	2.3	25.9	70.6	93.5	1.4	3.7	1.0	0.4
YCFC	1.3	2.1	49.1	47.5	92.4	1.6	4.9	0.8	0.3
DXYFC	2.2	2.2	1.2	94.5	93.5	1.1	4.2	0.8	0.5
DYCFC	2.4	2.0	1.3	94.2	93.2	1.0	4.5	0.8	0.4

[a]By difference.

model (RPM) and two modified RPMs, and the kinetic parameters were obtained. The aim is to investigate the gasification characteristics of fine chars and provide more useful information for designing and operating the integrated AFB-entrained flow gasifier.

2. EXPERIMENTAL SECTION

2.1. Raw Materials and Sample Preparation. Two kinds of fine chars separated from the secondary cyclone of a pilot-scale AFB were selected in this study: Xiangyuan bituminous fine char (XYFC) and Yangcheng anthracite fine char (YCFC). The operational temperature for these fine chars was about 1000 °C, while XYFC derived from a lower pressure (0.6 MPa) than YCFC (2.1 MPa). The gasification mediums of fine chars were H_2O/O_2, while more operation parameters can be consulted elsewhere.[17] The fine chars sieved to fractions of a particle diameter <125 μm (>80 wt %) were used as the experimental samples. To evaluate the influences of ash/inorganic elements on the gasification reactivity, two demineralized fine char samples were acid-washed by HF and HCl according to the criterion of GB/T 7560-2001 (Chinese Standard) and denoted as DXYFC and DYCFC, respectively.

Two rapid pyrolysis coal chars corresponding to these two coals were prepared in a fixed-bed reactor.[18] In brief, about 10 g of coal sample (<125 μm) was loaded in a crucible and maintained within the cooled zone of the reactor. After the reactor was heated to 900 °C under a N_2 atmosphere (150 mL/min), the crucible was quickly pushed into the heated zone for 30 min of pyrolysis. Then, the crucible was shifted to the cooled zone for 30 min, and the coal chars were obtained (designated as XYCC and YCCC). The heating rate of the coal samples was about 150 °C/s. The coal char samples were ground and sieved again to obtain particles smaller than 125 μm.

2.2. Property Tests of Samples. The proximate and ultimate analyses of raw coal and the resulting chars were conducted on the basis of Chinese Standard GB/T 212-2001 and GB/T 476-2001, respectively. The inorganic elements of raw and demineralized fine chars were measured by the inductively coupled plasma (ICP) spectrometer (Thermo iCAP 6300). Besides, the ash fusion temperature measurements were performed according to the Chinese Standard GB/T 219-1996.

A JSM-7001F scanning electronic microscope (SEM) was employed to provide the detailed surface morphology of fine char and coal char samples. The Brunauer–Emmett–Teller (BET) surface area of samples was obtained from N_2 adsorption by TriStar 3000 analyzers at −196 °C. Before the analysis, the samples were degassed under vacuum at 200 °C for 10 h. The micropore area and volume were calculated by the *t*-plot method, while the total pore volume was obtained from the amount adsorbed at 0.994 relative pressure. Moreover, a RIGAKU D/max-rB X-ray powder diffractometer was used to measure the X-ray intensities. Cu Kα radiation (40 kV, 100 mA) was used as the X-ray source, and samples were scanned over a 2θ range of angles from 10° to 80°, with a step size of 0.01°. The stacking height (L_c) of samples was calculated by the Scherrer formula.

2.3. Measurements of CO_2 Gasification Reactivity. The isothermal CO_2 gasification experiments were performed with a Setaram Setsys TGA under atmospheric pressure at the temperatures of 1000–1300 °C. In each experiment, an approximate 5 mg sample was placed in an alumina crucible (8 mm inner diameter and 5 mm height) and heated to the desired temperatures under a N_2 atmosphere (120 mL/min), with a heating rate of 30 °C/min. After being held under the desired temperature for 3 min, the temperature and weight of samples were approximately unchanged. Then, the gas was switched to CO_2 with the same flow rate, and the gasification reaction began. The weight loss of the sample was recorded every 5 s, and the repeatability was found to be excellent, with a relative standard deviation of less than 1.5%.

The carbon conversion X and gasification reaction rate r of samples were calculated by the following equations:

$$X = \frac{W_0 - W_t}{W_0 - W_\infty} \tag{1}$$

$$r = \frac{dW}{dt}\frac{1}{W_0 - W_\infty} = \frac{dX}{dt} \tag{2}$$

where W_0, W_t, and W_∞ represent the initial weight, the actual weight at a gasification time of t, and the left weight after being completely converted, respectively. The Savitzky–Golay method[19] with a two-degree polynomial model was used to smooth the gasification rate curves. The reaction rate curves (before and after smoothing) have the same number of data points as the carbon conversion curves. To distinguish the curves from different temperatures, the carbon conversion and reaction rate of every 0.1 carbon conversion were displayed in the figures.

The reactivity index R_s (min^{-1}), proposed by Takarada et al.,[20] was widely used to compare the reactivity between different samples. It is defined as

$$R_s = 0.5/\tau_{0.5} \tag{3}$$

where $\tau_{0.5}$ is the time needed when the carbon conversion reaches 0.5.

3. RESULTS AND DISCUSSION

3.1. Physical and Chemical Properties of Samples. The proximate and ultimate analyses in Table 1 show that the fixed carbon content, ash content, and chemical components of two coal chars are similar. In comparison to the coal chars, the fine chars that have been partially gasified have a lower fixed carbon content, especially for the YCFC (47.5%). The fixed carbon content of XYFC reaches up to 70.6%, suggesting the necessity of the regasification of fine chars. In addition, the fine chars are rich in ash content. The inorganic elements in ash, especially the alkali and alkaline earth metals (AAEMs, such as K, Na, Ca, and Fe), have catalytic effects on the gasifiacation reactivity. These inorganic elements can be effectively removed by acid wash. After demineralization, the ash content of DXYFC and DYCFC decreases to 1.2 and 1.3%, respectively, and most of

dx.doi.org/10.1021/ef4002296 | Energy Fuels 2013, 27, 2422–2430

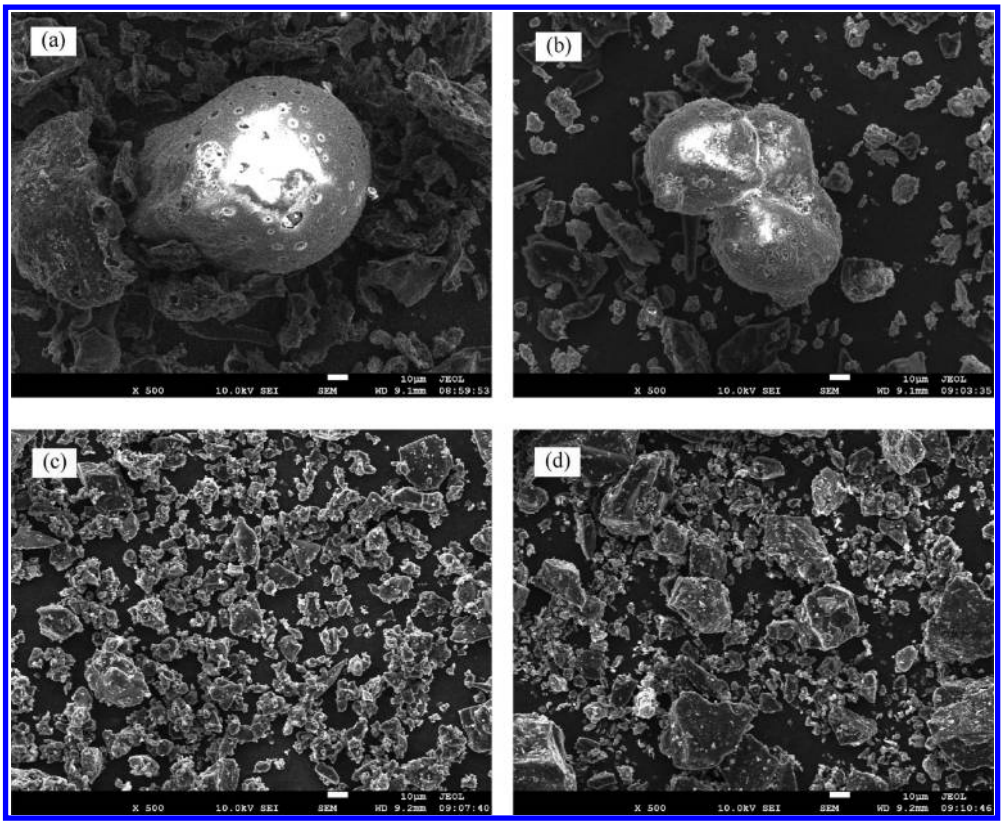

Figure 1. SEM micrographs of fine chars and coal chars: (a) XYFC, (b) YCFC, (c) XYCC, and (d) YCCC.

Table 2. Inorganic Elements and Ash Fusion Temerpatures of Fine Chars

	inorganic analysis (μg/g, air-dry basis)							ash fusion temperature (°C)		
sample	Si	Al	Fe	Ca	Mg	K	Na	DT[a]	ST[a]	FT[a]
XYFC	56817	52715	4734	9716	4042	1274	577	1500	>1500	>1500
YCFC	104859	99560	13116	20321	5268	2943	1528	1500	>1500	>1500
DXYFC	1786	1742	408	523	330	23	160			
DYCFC	1980	2306	661	413	457	35	151			

[a]DT, deformation temperature; ST, soften temperature; and FT, flow temperature.

the AAEMs are removed. Consequently, the influences of ash/AAEMs on the gasification reactivity of demineralized fine chars could be neglected.[21,22]

The SEM micrographs could provide surface morphology of fine char and coal char samples. As seen from Figure 1, two fine chars agglomerate to form larger spherical-like particles, which may be the result of the higher temperature in the central tube zone of the AFB.[23] The agglomeration can also be accelerated by the higher operating pressure of the gasifier.[15] In contrast, no agglomeration can be found for the coal chars deriving from a lower operating temperature and pressure. Besides, the fine chars exhibit more pores than the irregular and sharp-edged coal chars, which will be quantitatively discussed on the basis of N_2 adsorption.

The pore structure analyses of fine chars and coal chars are listed in Table 3, where the BET surface area, micropore area, total pore volume, and micropore volume were obtained by N_2 adsorption.[24,25] The surface area and pore volume reveal that the fine chars are more porous than the coal chars. For example, YCFC has the largest BET surface area and total pore volume (274 m^2/g and 0.152 cm^3/g, respectively), which are much larger than those of YCCC (13 m^2/g and 0.012 cm^3/g, respectively). The high porosity of fine chars could be explained

Table 3. Pore Structure Analyses of Fine Chars and Coal Chars

sample	BET surface area (m^2/g)	micropore area (m^2/g)	total pore volume (cm^3/g)	micropore volume (cm^3/g)
XYCC	<1	<1	0.003	<0.001
YCCC	13	10	0.012	0.005
XYFC	48	20	0.040	0.009
YCFC	274	146	0.152	0.066

by the fact that the fine chars have been partially gasified and activated by steam in the gasifier. It had to be noticed that, after the pyrolysis process, YCCC became a highly dispersed powder, while XYCC particles were bound into a sponge-like cake. This behavior is a significant character of the coking process, which can be described as the caking property. The higher caking property of XYCC could suppress the release of volatile matter, which is similar to the effect of the pressure. Accordingly, less reactive "secondary chars" form on the char surface, and pores are blocked by the redeposition and repolymerization of volatile matter.[26,27] This is probably the

dx.doi.org/10.1021/ef4002296 | Energy Fuels 2013, 27, 2422−2430

main reason for the lower porosities of XY samples than YC samples.

With regard to the pore structure, the surface area could provide active sites for the reaction and the char gasification reactivity is considered to be proportional to the number of active sites. Furthermore, the pore size distribution would influence the diffusion of reactants and products. As demonstrated in Table 3, the micropore area and BET surface area of coal chars are nearly the same, although the difference is more significant for the fine chars. It indicates that the fine chars are richer in meso- and macropores than the coal chars.

The carbon crystalline structure is another significant property of carbonaceous materials. According to the XRD patterns (Figure 2), a broad 002 band, which is similar to the characteristic peak of graphite, is observed at approximately 25° and the corresponding stacking height (L_c) of the crystal lattice could be obtained. Obviously, the 002 peak of XYFC is sharper and higher than that of YCFC, which suggests the higher ordered crystalline structure and limited active sites at crystalline edges.[14] Previous studies indicated that the crystalline structures of coal chars were affected by the pyrolysis conditions, especially the temperature, pressure, and residence time.[24,28] However, Meng et al.[29] noted that the gasification temperature had fewer effects on the crystalline structure of biomass chars. From Figure 2, it can be found that the L_c values of coal chars and the corresponding fine chars are similar, which means that the crystalline structures of different samples are mainly controlled by the coal types. Additionally, the sharp peak at around 26.6° represents SiO_2, while the peaks at 16.4°, 33.2°, 33.2°, and 40.8° are mullite ($Al_6Si_2O_{13}$) and the peak at 31.3° is related to the presence of gehlenite ($2CaO{\cdot}Al_2O_3{\cdot}SiO_2$).[23]

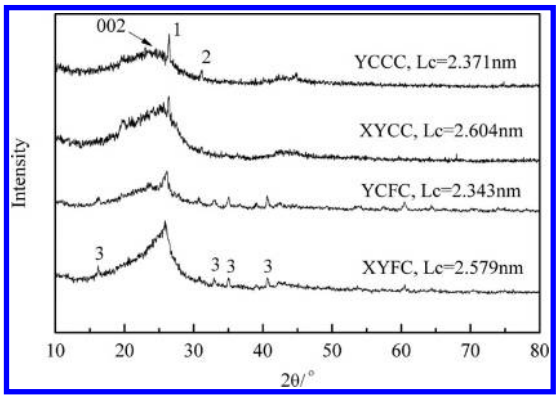

Figure 2. XRD patterns of fine chars and coal chars (1, quartz; 2, gehlenite; and 3, mullite).

According to the analysis results mentioned above, it could be concluded that the properties of fine chars and coal chars are markedly different, especially with respect to the pore structure. The influences of these properties on gasification reactivity will be investigated in the following section.

3.2. CO_2 Gasification Behaviors of Samples. *3.2.1. CO_2 Gasification Reactivity of Fine Chars and Other Samples.* YCFC is chosen as an example to study the effect of the temperature on the CO_2 gasification reactivity of the fine char in the temperature range of 1000−1300 °C. As shown in Figure 3, the time required to reach 0.9 carbon conversion is 36 min at 1000 °C, which decreases to 2 min at 1300 °C. It means that a high carbon conversion of fine chars could be obtained in a shorter time at higher temperatures. The reactivity indexes listed in Table 4 also suggest that the gasification reactivity of fine chars can be enhanced effectively by the increase of the temperature. That is to say, the high-temperature gasification of fluidized-bed gasifier fine chars is an attractive option.

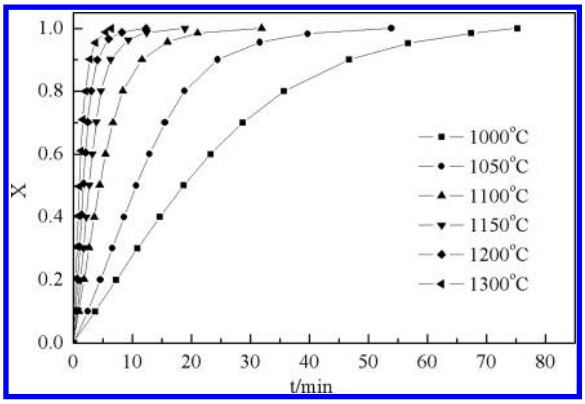

Figure 3. X−t curves of YCFC during CO_2 gasification at different temperatures.

Figure 4 presents the gasification rate r versus carbon conversion X of fine chars and other samples. It is noteworthy that all of the gasification rates first increase to a maximum and then gradually decline with the carbon conversion. This peak shape curve is related to the initial porosity and the variation of the pore structure during the gasification process. When the initial porosity is lower, the original blocked pores are opened in the initial stage, followed by widening of the micropore, coalescence of the neighboring pore, and collapse of the macropore.[12,30] This process lead to the accordance of the surface area and gasification rate. As obtained from section 3.1, the BET surface area of coal chars is extremely small; therefore, the gasification rate increases sharply at the initial stage (panels e and f of Figure 4). Besides, there are several differences in the term of gasification reactivity between different samples, which are affected by their ash/AAEMs content and physical properties. It will be discussed in more detail below.

3.2.2. Effects of Ash/AAEMs on the Gasification Reactivity of Fine Chars. It has been concluded that the inorganic elements, especially the AAEMs, have catalytic effects on the coal gasification.[31] The fine chars have been partially gasified and exhibit higher ash content; therefore, the effect of inherent minerals on gasification reactivity needs to be considered. The comparison between gasification rates of raw and demineralized fine chars is illustrated in Figure 5. Figure 5a shows that, under 1100 and 1200 °C, the reaction rate of DXYFC is lower than that of XYFC in the conversion range of $X < 0.7$ and $X < 0.5$, respectively, whereas the opposite result is observed in a higher conversion range. It demonstrates that the catalytic effect of AAEMs is significant in the former range; however, the ash will be enriched with the carbon conversion, and the thickness of the ash layer certainly increases, which would inhibit the gas diffusion rate in the range of higher carbon conversion and, hence, reduce the reaction rate.[32] However, Figure 5b presents that the reaction rate of YCFC is higher than that of DYCFC in the overall conversion range, which means a prominent catalytic effect. From Table 2, it can be found that the AAEMs contents of two fine chars are proportional to their ash content: the higher the ash content, the more the AAEMs and the better the catalytic effect.

dx.doi.org/10.1021/ef4002296 | Energy Fuels 2013, 27, 2422−2430

Table 4. Reactivity Indexes of Fine Chars and Other Samples

	R_s (min^{-1})					
temperature (°C)	XYCC	YCCC	XYFC	YCFC	DXYFC	DYCFC
1000	0.0123	0.0188	0.0170	0.0267	0.0159	0.0189
1050	0.0216	0.0394	0.0294	0.0469	0.0264	0.0382
1100	0.0375	0.0678	0.0599	0.1116	0.0481	0.0702
1150	0.0474	0.0924	0.0864	0.1838	0.0669	0.1066
1200	0.0582	0.1116	0.1250	0.2890	0.0992	0.1818
1250	0.0705	0.1276	0.1678	0.4505	0.1563	0.2525
1300	0.1010	0.1412	0.2381	0.4902	0.2674	0.2994

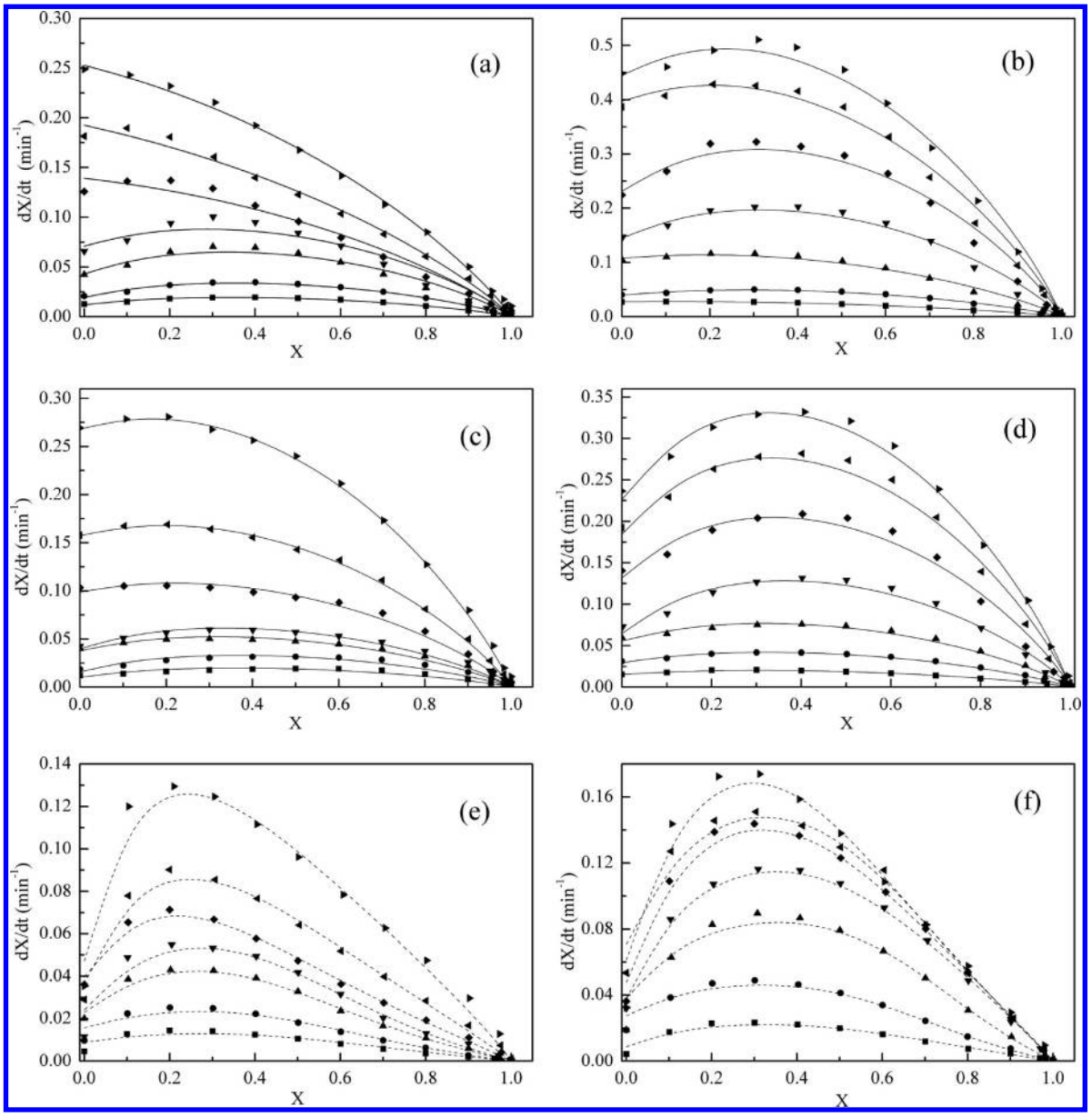

Figure 4. Gasification rates and fitting curves of samples: (a) XYFC, (b) YCFC, (c) DXYFC, (d) DYCFC, (e) XYCC, and (f) YCCC (■, 1000 °C; ●, 1050 °C; ▲, 1100 °C; ▼, 1150 °C; ♦, 1200 °C; ◀, 1250 °C; ▶, 1300 °C; —, fitting curves of RPM; and - - -, fitting curves of S-MRPM).

Figure 5a also shows that the gasification rate of XYFC is lower than that of DXYFC in the overall conversion range under 1300 °C. It has been found that the XYFC residues stick to the crucible after the gasification under 1300 °C. A comparison between Figure 6 (SEM image of the XYFC residue at 1300 °C with a carbon conversion of 0.5) and Figure 1a shows that, for the XYFC residues, tiny droplets and no pores are present on the smooth surface of the spherical particle.[33] These suggest that the ash of XYFC fused under 1300 °C. The fused ash will coat the unreacted carbon, inhibit the diffusion of the gasifying agent, and decrease the gasification rate of XYFC.[34]

dx.doi.org/10.1021/ef4002296 | Energy Fuels 2013, 27, 2422−2430

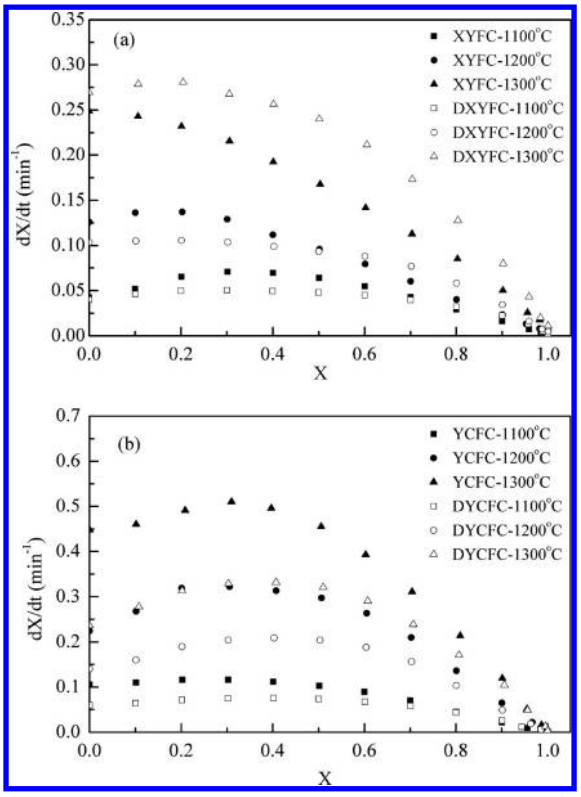

Figure 5. Reaction rate comparison of the raw and demineralized fine char samples: (a) XYFC and DXYFC and (b) YCFC and DYCFC.

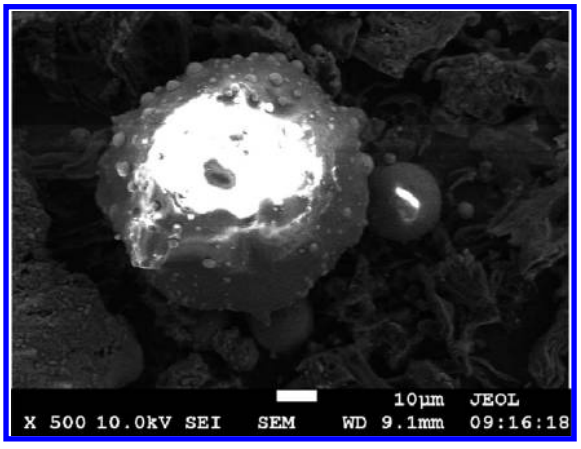

Figure 6. SEM image of the XYFC residue at 1300 °C with a carbon conversion of 0.3.

3.2.3. Gasification Reactivity Comparison and Influence Factors. Table 4 presents that the gasification reactivity of bituminous XYFC is lower than that of higher rank anthracite YCFC, which is inconsistent with the previous study that the gasification reactivity decreases as the coal rank increases.[35] Ochoa et al.[12] summarized the main causes for the different reactivity of coal chars as follows: the concentration of active sites, the rate of the gasifying agent accessing the active site, and the catalytic effects of inherent minerals. Results shown in Tables 1 and 2 suggest that the better reactivity of YCFC could be ascribed to the catalytic effect of the higher ash/AAEMs content. However, the CO_2 gasification reactivity of DYCFC is still higher than that of DXYFC. As mentioned above, YCFC has a lower ordered crystalline structure and larger BET surface than XYFC, which means that the gasification reactivity of different fine chars is mainly influenced by the surface area and crystalline structure.[14−16] In comparison to the coal chars, the higher gasification reactivity of fine chars is probably due to the larger surface area and higher ash content. Meanwhile, more meso- and macropores of fine chars are also beneficial to CO_2 gasification.[25,34]

3.3. Kinetic Analyses. Many kinetic models have been used to simplify the gasification reactions, such as the homogeneous model,[36] shrinking core model,[37] RPM,[38] and modified random pore models (MRPMs).[39] From Figure 4, it could be clearly observed that there is a maximum for the gasification rate. In these models, only the RPM could interpret this phenomenon very well.[13] The function of RPM is described in eq 4

$$r = \frac{dX}{dt} = K(1 - X)\sqrt{1 - \varphi \ln(1 - X)} \tag{4}$$

where K is the reaction rate constant and φ is a dimensionless parameter including the initial pore structure. Theoretically, K is equal to the initial reaction rate, and φ reflects the acuteness of peaks.

The nonlinear least-squares method in the MATLAB curve fitting tool box was used to estimate the rate constant K and structure parameter φ.[40] In general, the gasification of raw and demineralized fine chars could be predicted by the RPM (solid lines in panels a−d of Figure 4). Most of the correlation coefficients (R^2) of RPM are higher than 0.98, except for several specific conditions (Table 5). Subsequently, a conversion term with two dimensionless parameters, called c and p, are added to modify the original RPM. The function of MRPM is shown as follows:

$$r = \frac{dX}{dt} = K(1 - X)\sqrt{1 - \varphi \ln(1 - X)}\,(1 + (cX)^p) \tag{5}$$

where c is a dimensionless constant and p is a dimensionless power law constant. If $c = 0$, it becomes the same as the RPM.

Table 5. Fitting Parameters of RPM, MRPM, and S-MRPM

model	sample	K (min^{-1})	φ	c	p	R^2
RPM	DXYFC-1000 °C	0.0102	18.43			0.9728
	DXYFC-1050 °C	0.0157	22.21			0.9795
	XYCC-1200 °C	0.0527	3.81			0.9374
	XYCC-1300 °C	0.0587	17.42			0.9346
MRPM	DXYFC-1000 °C	0.0120	2.49	1.87	1.09	0.9982
	DXYFC-1050 °C	0.0195	2.64	1.91	1.08	0.9980
S-MRPM	XYCC-1200 °C	0.0397	22.00	1.60	1.96	0.9978
	XYCC-1300 °C	0.0473	65.76	1.44	1.40	0.9940

dx.doi.org/10.1021/ef4002296 | Energy Fuels 2013, 27, 2422−2430

These two parameters take the effects of inherent minerals on the pore structure or pore structure changing with conversion into consideration.[39,41] It can be found from Table 5 that the K values of MRPM become higher and closer to the initial reaction rate compared to those of RPM. The larger c and smaller φ values in MRPM suggest that the residual AAEMs in DXYFC are difficult to be released and lead to a maximum reaction rate in the high conversion range.[39] The correlation coefficients in Table 5 and dash lines in Figure 7a indicate that the MRPM performs better than the RPM.

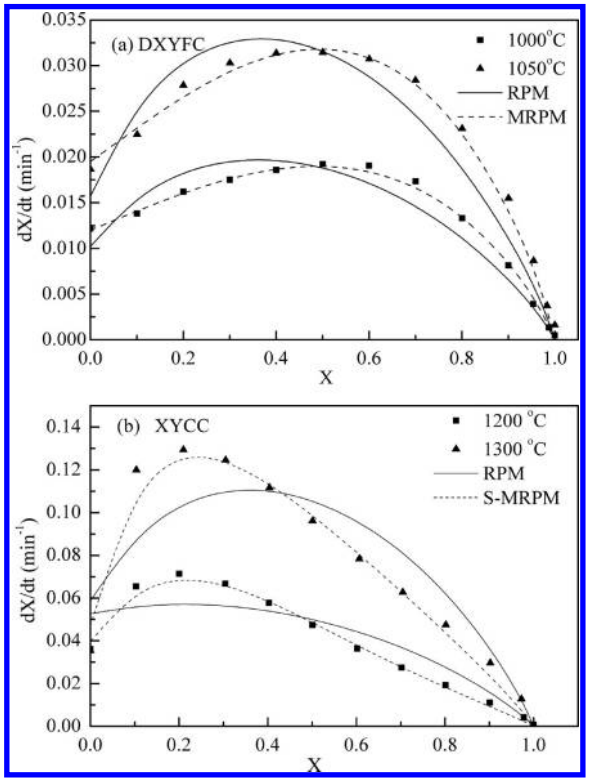

Figure 7. Fitting result comparisons of RPM, MRPM, and S-MRPM on gasification rates: (a) DXYFC and (b) XYCC.

Furthermore, the gasification rate of coal chars exhibits a peak value at a lower carbon conversion around 0.2 because of the smaller surface area. On the basis of the MRPM, a shifted-MRPM (S-MRPM) is developed to fit this variation, where the conversion term $(1 + (cX)^p)$ of MRPM is changed from multiplication to division.[24]

$$r = \frac{dX}{dt} = \frac{K(1 - X)\sqrt{1 - \varphi \ln(1 - X)}}{1 + (cX)^p} \quad (6)$$

Panels e and f of Figure 4 illustrate the fitting results of coal chars by S-MRPM, and the comparisons of RPM and S-MRPM for XYCC are shown in Figure 7b. Clearly, the S-MRPM performs very well with much higher correlation coefficients (>0.99). The largest φ values listed in Table 5 are in accordance with the sharp peaks of coal char samples. The better fitting results of S-MRPM and MRPM than that of RPM suggest that the gasification is not only affected by the initial pore structure but also the inherent minerals and variation of the pore structure in the process.

It has been pointed out that the K values in these models are close to the initial gasification rate dX/dt $(X = 0)$. However, the switch of gas results for dX/dt $(X = 0)$ obtained from the TGA is not accurate.[24,42] Here, the gasification rates at a conversion of 0.5 are taken as the basis, and the Arrhenius plots of ln $r_{0.5}$ versus $1/T$ are presented in Figure 8. The activation energy E_a

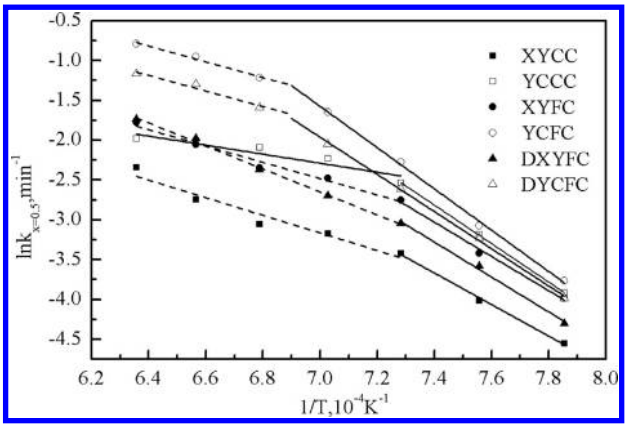

Figure 8. Arrhenius plots of samples in the temperature range of 1000−1300 °C.

and the pre-exponential factor A_0 could be calculated by the Arrhenius equation, and the results are listed in Table 6. The

Table 6. Kinetic Parameters of Samples at the Gasification Temperatures of 1000−1300 °C

	lower temperature range (<critical temperature)		higher temperature range (>critical temperature)	
sample	E_a (kJ/mol)	A_0 (min^{-1})	E_a (kJ/mol)	A_0 (min^{-1})
XYCC	164.46	5.83×10^4	91.85	96.70
YCCC	200.67	3.60×10^6	47.14	5.37
XYFC	178.68	3.90×10^5	85.04	107.66
YCFC	215.52	1.57×10^7	82.33	250.09
DXYFC	182.35	4.21×10^5	120.09	1.74×10^3
DYCFC	194.18	1.77×10^6	81.46	161.72

results show that the Arrhenius curves of YCFC and DYCFC can be divided into two stages by a critical temperature at 1175 and 1100 °C for other samples. The apparent activation energies of fine chars range from 178.68 to 215.52 kJ/mol below the critical temperature and about 85 kJ/mol above the critical temperature, which means that the activation energy in the high-temperature range is about half of that in the low-temperature range. This appears to result from pore diffusion. Lin et al.[34] found that the Thiele modulus M_T at 1000 °C was 0.17 ($M_T < 0.4$), where the pore diffusion resistance could be neglected. However, the pore diffusion would strongly influence the reaction rate when M_T was up to 7.65 ($M_T > 4$) at 1300 °C, and the observed activation energy was approximately half of the true activation energy. The kinetic parameters in this paper demonstrate that the chemical reaction is the controlling step in the lower temperature range for the gasification of fine chars, while in the higher temperature range, the gasification is influenced by strong pore diffusion resistance.[15,42]

4. CONCLUSION

The principal results are summarized as follows: (1) The fluidized-bed gasifier fine chars still contain a higher carbon content of 47−71%. The ash content and surface area of fine

dx.doi.org/10.1021/ef4002296 | Energy Fuels 2013, 27, 2422−2430

chars are higher than those of their corresponding rapid pyrolysis coal chars. There are agglomerates for the fine chars, while the carbon crystalline structures of fine char and coal char are similar. (2) The gasification reactivity of fine chars increases with the rise of the temperature, which confirms the feasibility of the regasification of fine chars in an entrained flow gasifier at higher temperatures. The AAEMs have a catalytic effect on gasification reactivity in the lower carbon conversion range; however, the enrichment of ash in the latter range decreases the reactivity. The ash melting at an elevated temperature (1300 °C for the XYFC) also reduces the gasification reactivity. In addition to the AAEMs, the gasification reactivity of different fine chars is mainly affected by their pore and crystalline structure. (3) The MRPM and S-MRPM describe the gasification better than RPM, while the gasification rate exhibits a maximum in a higher or lower conversion range. Gasification shifts from chemical reaction control to gas diffusion control with the increase of the temperature, and the activation energy in the high-temperature range is nearly half of that in the low-temperature range.

■ AUTHOR INFORMATION

Corresponding Author

*Telephone: +86-0351-2021137. E-mail: fyt@sxicc.ac.cn.

Notes

The authors declare no competing financial interest.

■ ACKNOWLEDGMENTS

The work is financially supported by the Strategic Priority Research Program of the Chinese Academy of Sciences (XDA07050100), the National Natural Science Foundation of China (21106173), and the Special Foundation for Young Scientists of the Institute of Coal Chemistry, Chinese Academy of Sciences (2011SQNRC01).

■ REFERENCES

(1) Meng, X. M.; de Jong, W.; Fu, N. J.; Verkooijen, A. H. M. Biomass gasification in a 100 kW_{th} steam−oxygen blown circulating fluidized bed gasifier: Effects of operational conditions on product gas distribution and tar formation. *Biomass Bioenergy* **2011**, *35* (7), 2910−2924.

(2) Lin, C. L.; Peng, T. H.; Wang, W. J. Effect of particle size distribution on agglomeration/ defluidization during fluidized bed combustion. *Powder Technol.* **2011**, *207* (1−3), 290−295.

(3) Qu, L. Q. Progress of research in the fluidized bed coal gasification technology. *Coal Convers.* **2007**, *30* (2), 81−85.

(4) Mondal, P.; Dang, G. S.; Garg, M. O. Syngas production through gasification and cleanup for downstream applications—Recent developments. *Fuel Process. Technol.* **2011**, *92* (8), 1395−1410.

(5) Fang, Y. T.; Tang, Z.; Li, M.; Zhang, J. M.; Wang, Y. Study on gasification reactivity of fine char from fluidized bed gasifier 1. The gasification reactivity difference between fine char and coal char made from laboratory. *J. Fuel Chem. Technol.* **1996**, *24* (2), 143−149.

(6) Higman, C.; Van der Burgt, M. *Gasification*; Gulf Professional Publishing: Oxford, U.K., 2003.

(7) Wu, J. H.; Fang, Y. T.; Peng, H.; Wang, Y. A new integrated approach of coal gasification: The concept and preliminary experimental results. *Fuel Process. Technol.* **2004**, *86* (3), 261−266.

(8) Maroto-Valer, M. M.; Taulbee, D. N.; Hower, J. C. Characterization of differing forms of unburned carbon present in fine char separated by density gradient centrifugation. *Fuel* **2001**, *80* (6), 795−800.

(9) Izidoro, J. d. C.; Fungaro, D. A.; dos Santos, F. S.; Wang, S. Characteristics of Brazilian coal fly ashes and their synthesized zeolites. *Fuel Process. Technol.* **2012**, *97* (0), 38−44.

(10) Liu, H.; Luo, C. H.; Kato, S.; Uemiya, S.; Kaneko, M.; Kojima, T. Kinetics of CO_2/char gasification at elevated temperatures. Part I: Experimental results. *Fuel Process. Technol.* **2006**, *87* (9), 775−781.

(11) Liu, H.; Luo, C. H.; Toyota, M.; Uemiya, S.; Kojima, T. Kinetics of CO_2/char gasification at elevated temperatures. Part II: Clarification of mechanism through modelling and char characterization. *Fuel Process. Technol.* **2006**, *87* (9), 769−774.

(12) Ochoa, J.; Cassanello, M.; Bonelli, P.; Cukierman, A. CO_2 gasification of Argentinean coal chars: A kinetic characterization. *Fuel Process. Technol.* **2001**, *74* (3), 161−176.

(13) Zolin, A.; Jensen, A.; Pedersen, L. S.; Dam-Johansen, K.; Torslev, P. A comparison of coal char reactivity determined from thermogravimetric and laminar flow reactor experiments. *Energy Fuels* **1998**, *12* (2), 268−276.

(14) Kelebopile, L.; Sun, R.; Liao, J. Fly ash and coal char reactivity from thermo-gravimetric (TGA) experiments. *Fuel Process. Technol.* **2011**, *92* (6), 1178−1186.

(15) Gu, J.; Wu, S. Y.; Wu, Y. Q.; Li, Y.; Gao, J. S. Differences in gasification behaviors and related properties between entrained gasifier fine char and coal char. *Energy Fuels* **2008**, *22* (6), 4029−4033.

(16) Xu, S. Q.; Zhou, Z. J.; Gao, X. X.; Yu, G. S.; Gong, X. The gasification reactivity of unburned carbon present in gasification slag from entrained-flow gasifier. *Fuel Process. Technol.* **2009**, *90* (9), 1062−1070.

(17) Liu, Z. Y.; Fang, Y. T.; Deng, S. P.; Huang, J. J.; Zhao, J. T.; Cheng, Z. P. Simulation of pressurized ash agglomerating fluidized bed gasifier using ASPEN PLUS. *Energy Fuels* **2012**, *26* (2), 1237−1245.

(18) Ren, H. J.; Zhang, Y. Q.; Fang, Y. T.; Wang, Y. Co-gasification behavior of meat and bone meal char and coal char. *Fuel Process. Technol.* **2011**, *92* (3), 298−307.

(19) Alciaturi, C. E.; Escobar, M. E.; de La Cruz, C.; Vallejo, R. Determination of chemical properties of pyrolysis products from coals by diffuse-reflectance infrared spectroscopy and partial least squares. *Anal. Chim. Acta* **2001**, *436* (2), 265−272.

(20) Takarada, T.; Tamai, Y.; Tomita, A. Reactivities of 34 coals under steam gasification. *Fuel* **1985**, *64* (10), 1438−1442.

(21) Eom, I. Y.; Kim, J. Y.; Lee, S. M.; Cho, T. S.; Yeo, H.; Choi, J. W. Comparison of pyrolytic products produced from inorganic-rich and demineralized rice straw (*Oryza sativa* L.) by fluidized bed pyrolyzer for future biorefinery approach. *Bioresour. Technol.* **2013**, *128* (0), 664−672.

(22) Ye, D. P.; Agnew, J. B.; Zhang, D. K. Gasification of a south Australian low-rank coal with carbon dioxide and steam: kinetics and reactivity studies. *Fuel* **1998**, *77* (11), 1209−1219.

(23) Li, F. H.; Huang, J. J.; Fang, Y. T.; Liu, Q. R. Fusibility characteristics of residual ash from lignite fluidized-bed gasification to understand its formation. *Energy Fuels* **2012**, *26* (8), 5020−5027.

(24) Yuan, S.; Chen, X. L.; Li, J.; Wang, F. C. CO_2 gasification kinetics of biomass char derived from high-temperature rapid pyrolysis. *Energy Fuels* **2011**, *25* (5), 2314−2321.

(25) Malekshahian, M.; Hill, J. M. Effect of pyrolysis and CO_2 gasification pressure on the surface area and pore size distribution of petroleum coke. *Energy Fuels* **2011**, *25* (11), 5250−5256.

(26) Zhuo, Y.; Messenböck, R.; Collot, A. G.; Megaritis, A.; Paterson, N.; Dugwell, D. R.; Kandiyoti, R. Conversion of coal particles in pyrolysis and gasification: Comparison of conversions in a pilot-scale gasifier and bench-scale test equipment. *Fuel* **2000**, *79* (7), 793−802.

(27) Zhu, W. K.; Song, W. L.; Lin, W. G. Effect of the coal particle size on pyrolysis and char reactivity for two types of coal and demineralized coal. *Energy Fuels* **2008**, *22* (4), 2482−2487.

(28) Li, C. Y.; Zhao, J. T.; Fang, Y. T.; Wang, Y. Pressurized fast-pyrolysis characteristics of typical Chinese coals with different ranks. *Energy Fuels* **2009**, *23*, 5099−5105.

(29) Meng, X. M.; Benito, P.; de Jong, W.; Basile, F.; Verkooijen, A. H. M.; Fornasari, G.; Vaccari, A. Steam−O_2 blown circulating fluidized-bed (CFB) biomass gasification: Characterization of different residual chars and comparison of their gasification behavior to thermogravimetric (TG)-derived pyrolysis chars. *Energy Fuels* **2012**, *26* (1), 722−739.

(30) Molina, A.; Mondragon, F. Reactivity of coal gasification with steam and CO_2. *Fuel* **1998**, *77* (15), 1831−1839.
(31) Miura, K.; Hashimoto, K.; Silveston, P. L. Factors affecting the reactivity of coal chars during gasification, and indexes representing reactivity. *Fuel* **1989**, *68* (11), 1461−1475.
(32) Wu, S. Y.; Gu, J.; Li, L.; Wu, Y. Q.; Gao, J. S. Effects of ash fusion on reaction activity of Shenfu chars at elevated temperatures. *Coal Convers.* **2006**, *29* (4), 41−45.
(33) Li, S.; Whitty, K. J. Physical phenomena of char−slag transition in pulverized coal gasification. *Fuel Process. Technol.* **2012**, *95*, 127−136.
(34) Lin, S. Y.; Hirato, M.; Horio, M. The characteristics of coal char gasification at around ash melting temperature. *Energy Fuels* **1994**, *8* (3), 598−606.
(35) Dutta, S.; Wen, C.; Belt, R. Reactivity of coal and char. 1. In carbon dioxide atmosphere. *Ind. Eng. Chem. Process Des. Dev.* **1977**, *16* (1), 20−30.
(36) Wen, C. Noncatalytic heterogeneous solid fluid reaction models. *Ind. Eng. Chem.* **1968**, *60* (9), 34−54.
(37) Levenspiel, O. *Chemical Reaction Engineering*, 3rd ed.; Wiley: New York, 1999.
(38) Bhatia, S.; Perlmutter, D. A random pore model for fluid-solid reactions: I. Isothermal, kinetic control. *AIChE J.* **1980**, *26* (3), 379−386.
(39) Zhang, Y.; Ashizawa, M.; Kajitani, S.; Miura, K. Proposal of a semi-empirical kinetic model to reconcile with gasification reactivity profiles of biomass chars. *Fuel* **2008**, *87* (4−5), 475−481.
(40) Gomma, I. A. High temperature steam gasification of solid wastes: Characteristics and kinetics. Ph.D Thesis, University of Maryland, College Park, MD, 2011.
(41) Zhang, Y.; Hara, S.; Kajitani, S.; Ashizawa, M. Modeling of catalytic gasification kinetics of coal char and carbon. *Fuel* **2010**, *89* (1), 152−157.
(42) Kajitani, S.; Hara, S.; Matsuda, H. Gasification rate analysis of coal char with a pressurized drop tube furnace. *Fuel* **2002**, *81* (5), 539−546.